

# Correspondence

## Micromanipulator Vision for Wafer Probing

R. V. DANTU, N. J. DIMOPOULOS, MEMBER, IEEE,  
R. V. PATEL, SENIOR MEMBER, IEEE, AND  
A. J. AL-KHALILI, SENIOR MEMBER, IEEE

**Abstract**—This paper presents an overview of a micromanipulator vision system for use in automating various functions during the testing of a wafer for semiconductor parameters and inspection of VLSI circuits. The challenging problems relating to positioning a probe and enabling a probe to touch a test pad automatically using vision feedback are studied and some solutions are proposed.

### I. INTRODUCTION

Recent developments in VLSI wafer design indicate a shift towards design for testability [2]. Today's VLSI circuits have greater area, more I/O pins and facilities on the circuit itself for both testing the circuit and estimating the parameters of the process. The semiconductor parameters obtained through tests during fabrication improve the monitoring of the ongoing process quality and therefore the yield. The need for such process control and its yield benefits are discussed in [1]. In performing these tests, probes are used to inject test vectors, to monitor signatures, or to check for continuity [2], [3].

Another focus of research activity has been the automated visual inspection of IC chips. The main emphasis of this research has been in feature extraction and registration, so that the position and orientation of the pads and the integrated circuit itself can be determined [4]–[6], [8]–[12]. Once these features have been identified for a particular component, they are either compared to standard templates to determine their integrity, or they are used to automatically position the component for further inspection or probing. Two very good surveys [13], [14] have outlined recent work in automated visual inspection, with emphasis on integrated circuit inspection and feature registration. Since the main objective of the research described in this paper is in recognizing two-dimensional features of a component under inspection, rather than the actual manipulation of the component itself (through, for example, probing or wire bonding), no attempt has been made to determine the existence and location of features (such as probes) above the essentially two-dimensional component.

We are presently developing a micromanipulator system for automating such high-resolution tasks as IC testing and IC wafer inspection. The system is expected to be fully automated using vision feedback. In this work we concentrate on the vision activities that are required to be performed by the micromanipulator in order to accurately determine the position and orientation of both the probes and the IC.

The system under development provides a flexible testing environment using computer vision techniques and intelligent micro-

manipulator control for different tests. It is assumed that the wafer under test is not necessarily in its proper orientation. It is required that certain probes be lowered automatically onto certain pads to inject test vectors and to read the results for analysis. The position and orientation of the test circuit, the test pads and the probes have to be uniquely identified with high resolution. The probes have to be lowered to touch the pads nondestructively. This accurate and sensitive operation has to be performed repeatedly without the intervention of a human operator. It is the purpose of micromanipulator vision to manipulate the probes through collision-free trajectories and place them on well-identified pads.

In this work, we are primarily interested in determining the position (especially the vertical distance from the target) of the tip of a probe so that it can be guided accurately to its target pad. Thus, this work is divided into two parts. Section II outlines standard image processing steps employed for efficient feature extraction and registration of the target integrated circuit. Section III presents a method of obtaining the vertical distance of the tip of a probe from its target pad. It also gives two different criteria through which one can establish whether a probe is in contact with its target.

#### A. The Experimental Setup

Our setup consists of a VLSI test station with a microscope, platform, probes, wafer chuck, and a  $256 \times 256$  CCD camera. Images can be captured through the microscope, displayed and transferred to back-end processors for further processing. The probes can be interfaced to a variety of analyzing equipment for signature or parameter analysis. By using motorized probes, a closed-loop setup can be established. Currently, our main research effort is in processing the acquired images to extract information about the position and orientation of the probe, wafer, and pads. In this work, we concentrate on ways of finding the distance of the probe from its target based solely on information extracted from the acquired images.

### II. LOW-LEVEL PROCESSING AND FEATURE EXTRACTION

The acquired images consist, in general, of regions containing highly regular geometrical patterns which correspond to the VLSI component geometry, as well as of one or more mostly triangular and much darker regions which correspond to the probes or their shadows projected on the surface of the VLSI component. The geometrical patterns correspond primarily to reflections from the metal layer and from other layers such as the polysilicon. At this stage of our research, we are primarily interested in the metal layer since it is the most visible one and also because both the test pads and the wire-bonding pads are implemented in this layer. The obtained image is first filtered to remove any periodic noise (Figs. 1 and 2), and then it is further smoothed by spatial averaging,<sup>1</sup> which removes the noise introduced by the bright through-the-lens illumination used. Fig. 3 shows a typical raw image. Its histogram can be seen in Fig. 4, and the histogram corresponding to the smoothed image is shown in Fig. 5. Averaging also tends to smooth out the image's histogram which now exhibits two easily discernible re-

<sup>1</sup>Given an  $N \times N$  image  $f(x, y)$ , the smoothed image  $g(x, y)$  is obtained by averaging the grey level values of the pixels of the original image contained in a predetermined neighborhood  $S(x, y)$  of  $(x, y)$

$$g(x, y) = \frac{1}{M} \sum_{n, m \in S(x, y)} f(n, m)$$

where  $M$  is the total number of points in the set  $S(x, y)$ .

Manuscript received March 8, 1988; revised March 5, 1989. This work was supported by the Natural Sciences and Engineering Research Council of Canada.

R. V. Dantu, R. V. Patel, and A. J. Al-Khalili are with the Department of Electrical and Computer Engineering, Concordia University, Montreal, Que., Canada.

N. J. Dimopoulos is with the Department of Electrical and Computer Engineering, University of Victoria, Victoria, B.C., Canada.

IEEE Log Number 8928238.

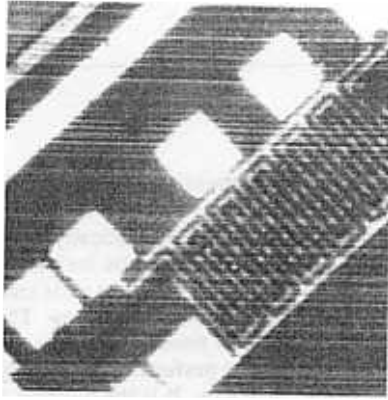


Fig. 1. Raw image from the camera.

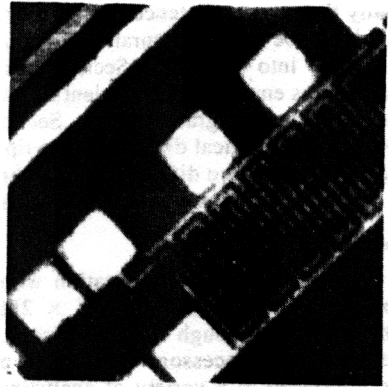


Fig. 2. Image after filtering periodic noise.



Fig. 3. Image of the probe touching the pad

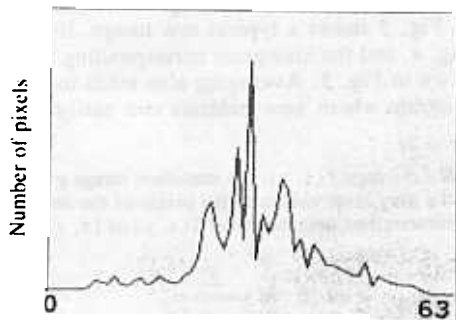


Fig. 4. Histogram of Fig. 3.

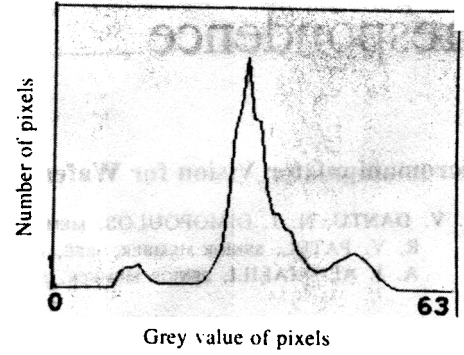


Fig. 5. Histogram of Fig. 3 after smoothing.

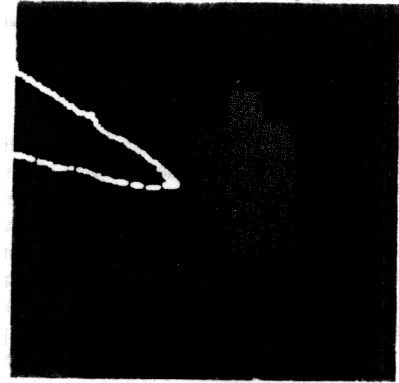


Fig. 6. Edge map of probe.

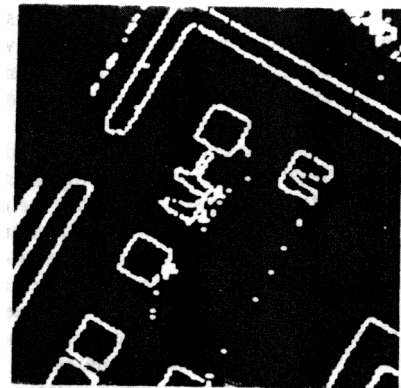


Fig. 7. Edge map of metal region in Fig. 3.

gions corresponding to the probes and the metalization regions. Next, thresholding is done to segment the patterns of interest corresponding to these regions. Such a thresholded image is used to get the edges. The Laplacian edge operator [7] is applied to the two regions to identify the edges. The results are given in Figs. 6 and 7.

The edge maps obtained from the above procedure are used for recognition of various patterns, orientations of the probe, orientations of the wafer, etc. Wafer orientation information is useful in aligning the probe with the pad and for further recognition of the elements of the die. We describe the detection of wafer orientation below. A Hough transform [7] of the edge map is taken. It is assumed that the patterning on the IC's is accomplished by using "Manhattan distances"; hence the prevailing patterns in the image are collections of short perpendicular line segments. Therefore, in the Hough transform, two peaks at a distance of  $90^\circ$  are observed. These peaks can be seen in Fig. 8 and correspond precisely to the

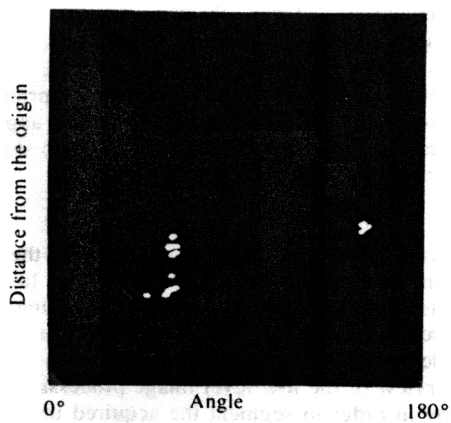


Fig. 8. Hough transform of Fig. 7.

two groups of perpendicular line segments existing in Fig. 3. The cross hairs in the camera eyepiece are taken as the base coordinate system for measurement.

The processing steps outlined above rely heavily on the fact that the images obtained correspond to essentially two-dimensional objects of high reflexivity. The only "dark" regions correspond to the probe (which being out of focus and of lower reflective index gives rise to a dark region) or its shadow. Simple thresholding therefore has proven adequate in distinguishing the patterns of interest.

In the next section, we concentrate on the distance of the probe from the surface of the target pad. This distance information is to be used during the automatic lowering of the probe until it touches the target pad.

### III. DETECTION OF TOUCH ON THE SURFACE

#### A. Calculation of Proximity

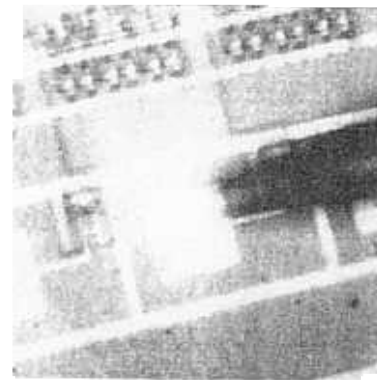
Touching a pad with a probe without scratching its surface, is a very sensitive operation on account of the thickness of the metalization layer ( $\sim 0.5 \mu\text{m}$ ). In order for the probe to make a good contact and not destroy the metalization layer, the probe's impact velocity and force must be accurately controlled. The estimation of the distance of the probe from the surface is therefore of paramount importance in successfully guiding the probe to its target pad.

In order to estimate the distance of the probe from the surface, we use the fact that the microscope has a very small  $f$  stop. Thus, if the microscope is focused on the surface of the IC, anything above this surface will be out of focus, and will appear "fuzzy" in the image. After identifying the tip of the probe, we measure the variance of the distribution of its pixels. The "fuzzier" the image is (i.e., the farther the tip of the probe is from the surface), the wider will be the variance of the pixel distribution.

The image of the probe when the probe is in focus, is obtained by determining its grey level threshold through the histogram of the image, as outlined in Section II. However, when the probe is out of focus, this method fails since the grey level values of the probe's pixels are very close to the ones of the background wafer. For such cases, we use the background image (the one where the probe is not present). From this background image, we subtract the image that contains the probe. The result is an image with pixels that have grey level equal to zero in regions where the probe is not present, and greater than zero in the probe region. One can easily segment the resulting image, and then use it as a mask in order to obtain the probe segment from the original image.

The mean  $\mu$  and variance  $\sigma$  of the probe pixel intensity values are calculated as follows:

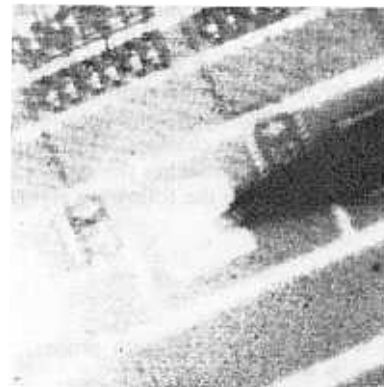
$$\text{mean } \mu = \sum_{y_s=y_1}^{y_s=y_2} y_s H(y_s) \quad \text{variance } \sigma^2 = \sum_{y_s=y_1}^{y_s=y_2} (y_s - \mu)^2 H(y_s)$$



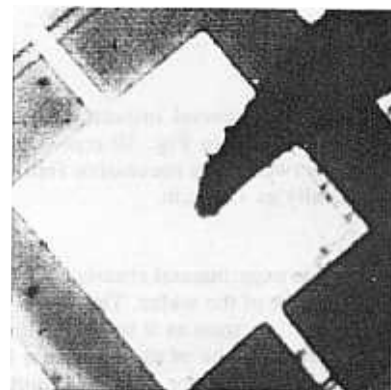
(a)



(b)



(c)



(d)

Fig. 9. (a)-(c) Sequence of images while probe is approaching the pad. (d) Probe touching the pad (magnified).

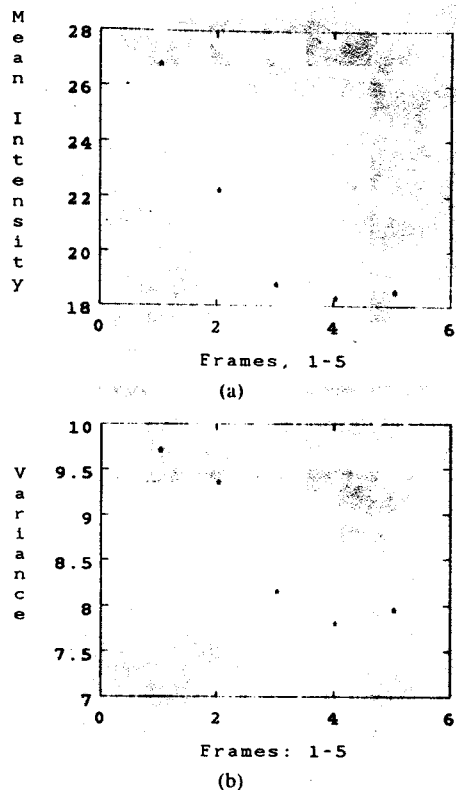


Fig. 10. (a) Mean intensity for different frames. (b) Variance of intensity for different frames.

where  $H(y_i)$  is the first-order histogram,  $y_i$  is the grey-level values of the pixels of the probe segment, and  $y_j$  is the number of grey levels.

Fig. 9(a)-(d) shows a sequence of images where the probe is approaching the wafer. As the probe approaches the surface (but does not quite touch it), it begins to come into focus and thus the variance of the pixel distribution changes. The changes in the variance and mean as the probe approaches the surface can be seen in Fig. 10 and are calculated using the following algorithm:

```

begin
  begin
    read(with_probe)
    read(without_probe)
    difference = without_probe - with_probe;
    if(difference >= tolerance)
      value = with_probe;
    else value = 0;
  end
  calculate_mean()
  calculate_variance();
end.

```

The frames are captured at several instants while the probe is approaching the wafer. Frame 4 in Fig. 10 represents the instant of touch. The distance between two successive frames in Fig. 10 is measured experimentally as 12.5  $\mu\text{m}$ .

### B. Test for Touching

We have established two experimental criteria for detecting when the probe touches the surface of the wafer. The first is based on the fact that the probe "slides" as soon as it touches the surface. The permitted "sliding" is found to be of the order of a few micrometers which corresponds to a difference in the position of the tip of the probe of about 15 pixels at the largest possible magnification. The dip at frame 4 in Fig. 10 corresponds to the instant of touch and frame 5 represents the sliding. The second method for prox-

imity measurement is used when the probe is away from the target, but in the vicinity of the field of focus. This is described briefly as follows. In Fig. 9(a), the image of the probe consists of two overlapping shapes that correspond to the image of the probe itself, and that of its shadow cast on the wafer. As the probe approaches and finally touches the surface of the target, these two shapes resolve into one indicating the touch.

### IV. CONCLUSIONS

In this work we have presented an overview of the micromanipulator system that we are currently developing for automating VLSI wafer testing. This research poses challenging problems in several different areas such as computer vision, artificial intelligence, parallel processing, and robotics. In this paper we have given an overview of the low-level image processing that we currently employ in order to segment the acquired image and obtain various features from it, e.g., the orientations of the wafer and the probes. We have also discussed the determination of the touch of a probe onto the wafer.

Reflection properties of the probe and the wafer vary according to the material of the tip and the technology of the process. We have tested the algorithm for touch using different types of tips such as tungsten and tungsten carbide, and with NMOS and CMOS processes. We have also used commercial dies, such as the Motorola 6805 and Intel 2708. We have been able to extract clean and accurate representations of the probes from integrated images in all our tests. All the algorithms have been tested with at least 15 sets of different data, each set having a minimum of five frames. In all these cases, touch was achieved without the surface being scratched. We are currently investigating the blurring functions of the microscope in order to deblur (focus) the probe when it is far from the wafer.

### REFERENCES

- [1] W. L. Engl, *Process and Device Modelling*. Amsterdam, Holland: North Holland, 1986.
- [2] T. W. Williams, *VLSI Testing*. Amsterdam, Holland: North Holland, 1986.
- [3] C. Beddoe-Stephens, "Semiconductor wafer probing," *Test Meas. World*, pp. 33-35, Nov. 1982.
- [4] K. L. Harris, P. Sandland, and R. M. Singleton, "Automated inspection of wafer patterns with applications in stepping projection and direct-write lithography," *Solid-State Technol.*, pp. 159-179, Feb. 1984.
- [5] M. L. Baird, "SIGHT-I: A computer vision system for automated IC chip manufacturing," *IEEE Trans. Syst., Man, Cybern.*, vol. SMC-8, pp. 133-139, 1979.
- [6] M. L. Baird, "EYSEE: A machine vision system for inspection of integrated circuit chips," in *Proc. IEEE Int. Conf. Robotics and Automation*, June 1985, pp. 444-448.
- [7] M. D. Levine, *Vision in Man and Machine*. New York: McGraw-Hill, 1985.
- [8] S. Kashioka, M. Ejiri, and Y. Sakamoto, "A transistor wire-bonding system utilizing multiple local pattern matching techniques," *IEEE Trans. Syst., Man, Cybern.*, vol. SMC-6, no. 8, Aug. 1976.
- [9] K. Igarashi, M. Naruse, S. Miyazaki, and T. Yamada, "Fully automated integrated circuit wire bonding system," in *Proc. 9th Int. Symp. Exposition on Industrial Robots* (Washington, DC), 1979, pp. 87-97.
- [10] M. Mese, I. Yamazaki, and T. Hamada, "An automatic position recognition technique for LSI assembly," in *Proc. 5th Int. Joint Conf. Artificial Intell.*, 1977, pp. 685-693.
- [11] Y. Y. Hsieh and K. S. Fu, "A method for automatic IC chip alignment and wire bonding," in *Proc. IEEE Comput. Soc. Conf. Pattern Recognition and Image Processing* (Chicago, IL), 1979, pp. 101-108.
- [12] Y. Y. Hsieh and K. S. Fu, "An automatic visual inspection system for integrated circuit chips," *Comput. Graphics and Image Process.*, vol. 14, pp. 293-343, 1980.
- [13] R. T. Chin and C. A. Harlow, "Automated visual inspection: A survey," *IEEE Trans. Pattern Analysis and Machine Intell.*, vol. PAMI-4, no. 6, pp. 562-565, Nov. 1982.
- [14] A. M. Wallace, "Industrial applications of computer vision since 1982," *Proc. Inst. Elec. Eng.*, vol. 135, pp. 117-136, May 1988.